High Altitude Radiation Detector (HARD): Integration of Undergraduate Research into Senior Design and Lessons Learned

Dr. Wookwon Lee, Gannon University

Wookwon Lee, P.E. received the B.S. degree in electronic engineering from Inha University, Korea, in 1985, and the M.S. and D.Sc. degrees in electrical engineering from the George Washington University, Washington, DC, in 1992 and 1995, respectively. He is currently on the faculty of the Department of Electrical and Computer Engineering at Gannon University, Erie, PA. Prior to joining Gannon, he had been involved in various research and development projects in industry and academia for more than 15 years.

Dr. Nicholas B. Conklin, Gannon University

Nicholas B. Conklin received a B.S. in applied physics from Grove City College in 2001, and a Ph.D. in physics from Penn State University in 2009. He is currently an assistant professor in the Physics Department at Gannon University, Erie, PA.

High Altitude Radiation Detector (HARD): Integration of Undergraduate Research into Senior Design and Lessons Learned

Abstract

An interdisciplinary undergraduate research project conducted as part of an ECE senior design is discussed. The focus of the research project was on aspects of physics, particularly on arrivals of cosmic rays in the so-called "east-west" angular asymmetry. In collaboration with NASA's Columbia Scientific Balloon Facility (CSBF) and other universities developing scientific ballooning payloads, a sophisticated scientific payload was designed to study how the angular asymmetry and intensity of cosmic rays changes with altitude, as well as conducting a high-quality, long-exposure measurement at balloon-float altitudes for about 10 hours. The payload was designed by following a top-down design approach: initially establishing engineering requirements of the payload for the experiment, carrying out functional decomposition, and actual laboratory design of subsystems by student team members enrolled in the Electrical and Computer Engineering (ECE) program at the University. The project team consisted of six undergraduate students (three seniors and three sophomores) from the ECE department and two faculty advisors from the ECE and Physics departments. The payload was certified flight-ready after integration and vacuum testing at CSBF with all modules functioning properly. Unfortunately, the payload failed to collect the desired cosmic-ray data during flight; however, all other parts of the design functioned as expected. Overall, adopted as a senior design project for an academic year, this project was a considerable success from a student education standpoint. Further details are provided on project design, team structure and collaboration, experimental details, and lessons learned, particularly on promoting student learning and improving its outcomes.

1. Overview of the Project

The Earth's magnetic field deflects cosmic-ray trajectories from a straight line. Due to the fact that cosmic rays are predominantly positively charged, this results in more particles arriving from the west than from the east. This "east-west" asymmetry has been investigated in the past at ground level. The goal of the project was to design and launch a small experimental payload to investigate how the "east-west" angular asymmetry changes with altitude, as the cosmic ray flux transitions from mostly secondary particles near the ground level to mostly primary cosmic rays near balloon-float altitudes. Additionally, this project intended to study how the intensity of cosmic rays changes with altitude, based on measurements of cosmic ray intensity from multiple arrival directions, providing a more complete picture of the high-altitude radiation environment caused by cosmic rays.

To achieve the project goal, a payload integrating various subsystems for cosmic-ray detection and event processing has been designed in a top-down design approach: initially establishing engineering requirements of the payload for the experiment, carrying out functional decomposition, and actual laboratory design of subsystems by student team members from the Electrical and Computer Engineering (ECE) department. Figure 1 shows the functional block diagram of the payload for the experiment, and Figure 2 shows a completed, sealed payload
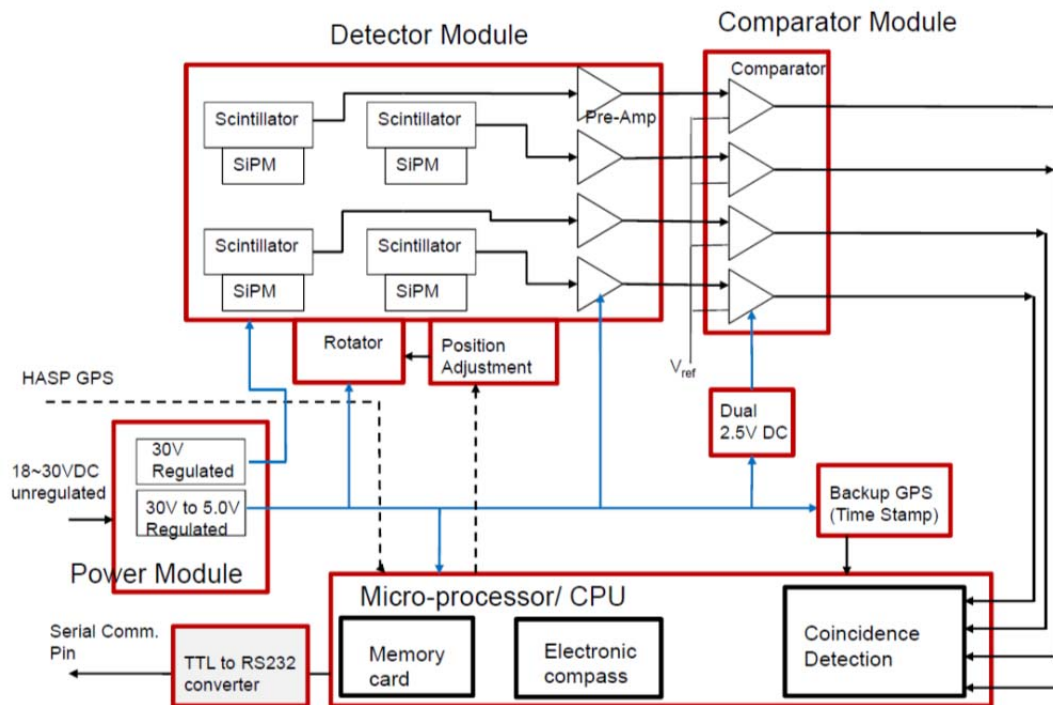
Figure 1. Overall functional block diagram for cosmic ray measurement

waiting for thermal and vacuum testing at NASA's Columbia Scientific Balloon Facility (CSBF) site. An exploded view of the recovered payload after flight is shown in Figure 3.

The student team primarily consisted of a total of six ECE undergraduate students including three seniors and three sophomores, and two faculty advisors from ECE and Physics department. For a short period of time during the summer 2011, a graduate student participated in the laboratory experiment to assist the team.

This project was initiated and formulated as a response to the Call for Payloads[1] from one of NASA's State Space Grant Consortia. As such, to some extent, the final project deadline and key design requirements for proper integration into the High Altitude Student Platform (HASP) were set. Along the course of the design activities, the team followed the schedule posted by the program director for the launch vehicle, HASP in Louisiana. As part of the requirements, the team delivered all monthly status reports from January 2012 to November 2012 on design activities for payload subsystems, a Payload Specification & Integration Plan (PSIP), Flight Operation Plan (FLOP), and on-site payload integration at the CSBF lab, as well as post-balloon launch activities.

2. Payload Subsystems

The key subsystems of the payload are the detector module, comparator module, coincidence detector, micro-processor/CPU, and power module. A brief description of each module is given below.
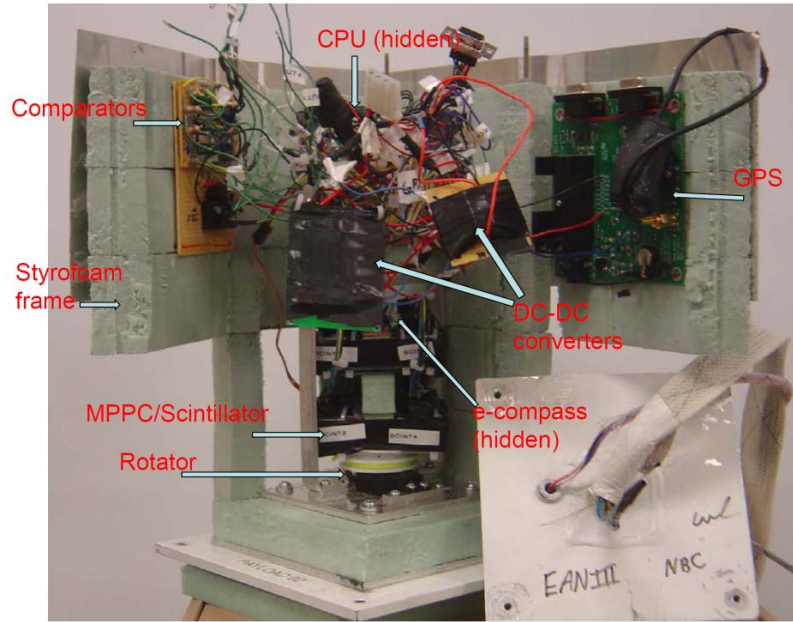
Figure 2. A completed, sealed payload

Figure 3. Interior view of GU-HARD-PL02

2.1. Detector Module

Four active detector elements are arranged in a square for detection of cosmic rays in the east-west plane. In this arrangement, a cosmic ray arriving from the east or west at the appropriate angle will traverse two detector elements simultaneously. Each active detector element consists of a Photonique SSPM 0905V13MM silicon photomultiplier (SiPM)[2] attached via optical epoxy to a $3 \times 3 \times 1\ cm^3$ CsI(TI) scintillating crystal, as shown in Figure 4(a). When a charged particle traverses the scintillator, a short (~1 µs) flash of light is emitted that is converted into an electric pulse by the SiPM and amplified for further processing. To artificially supply light to the scintillator for lab testing purposes, a green LED is also attached to the scintillator.

The scintillators are wrapped in Teflon tape to reflect stray photons back in, increasing the number of photons detected by the SiPM, and then in electrical tape to block outside light. A wrapped scintillator is shown in Figure 4(b). Each SiPM is connected to a pre-amplifier, also visible in the photos. The pre-amplifier generates a negative pulse with a magnitude ranging from 0 to about -1.0V depending on the number of photons impinging on the SiPM. The advantage of using SiPMs over traditional photomultiplier tubes (PMTs) is that they only require a very low (~30V) bias voltage, as opposed to the ~1 kV require by PMTs. This eliminates the need to pot the electronics in a dielectric, which is required with PMTs in near vacuum applications.
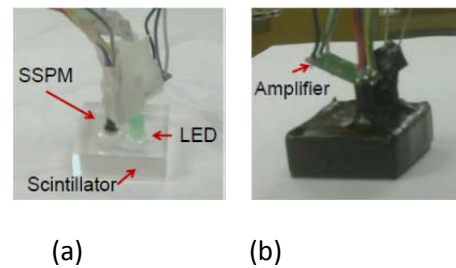

(a)   (b)

Figure 4. Detector module: (a) photo diode and scintillator (b) fully wrapped with a preamplifier

One challenge of working with the SiPM units is that the signals generated are very short. The pre-amplifiers have a typical rise time of 5 ns[3], although the long decay time of the CsI(TI) crystal results in pulses with a width on the scale of 1 µs. To detect such short pulses requires fast electronics. An application circuit of the pre-amplifier used for the detector module is shown in Figure 5 where capacitors C1 and C2 have a typical value of 10 nF.
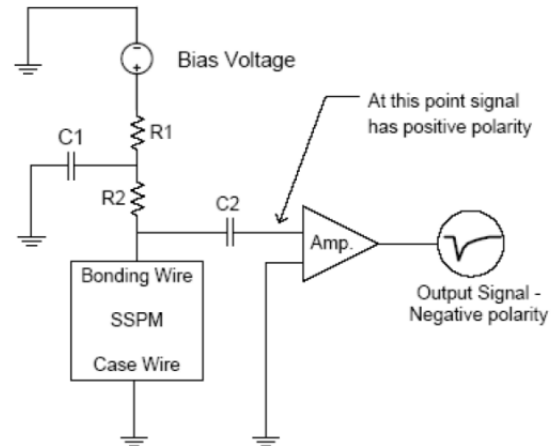

Figure 5. Application circuit diagram of the pre-amplifier for SiPM[3]

In order to detect the east-west asymmetry, the detector must be oriented so that the scintillator lies in the east-west plane. Given that the HASP instrument rotates during the flight, an HMC6352 electronic compass[4] is used to determine the orientation of the detector module. When the orientation of the payload drifts more than 10° from the desired orientation, a servo motor is used to adjust the detector. The completed detector subsystem integrated with the rotator subsystem is shown in Figure 6.

2.2.   Comparator Module

Each SiPM unit outputs a voltage proportional to the number of detected photons. However, this voltage signal is small and negative. This signal is inverted and amplified by an AD8616 inverting OP amp with a high voltage gain and large bandwidth operating at a frequency of up to 20 MHz[5]. A typical LM741 OP amp was tried first but did not have sufficient gain at high frequencies.

2.3.   Coincidence Detector

The output of the comparator module is connected to the digital inputs of the microprocessor. To monitor for a coincidence in two or more SiPM modules at a time, the microprocessor polls these inputs approximately once each microsecond. When this condition is met, the SiPM modules that contributed to the coincidence are identified and stored for later analysis.

2.4.   Microprocessor/CPU

A chipKIT Uno32 Prototyping Platform[6] is used as the main microprocessor module. This board provides a number of functions, including poling the digital I/O pins to determine whether a coincidence has been met; serial communication with HASP; monitoring temperature, detector orientation and GPS
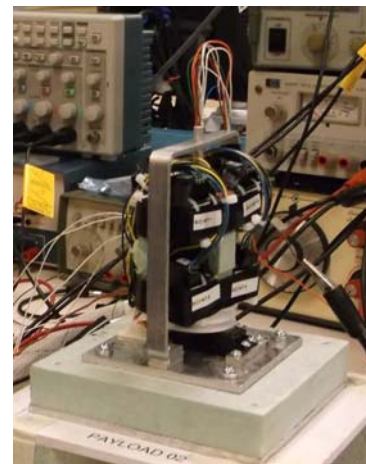

Figure 6. Fully assembled detector module with the rotator module

time; controlling the servo to adjust detector orientation; and recording data to an SD card.

The following list of subroutines implemented in the microprocessor illustrates the necessary functionality:

- FlightCode.pde: Main program to integrate all subroutines and download the codes onto the microcontroller
- M01_GPS.pde: for GPS-related functions
    - void SetupGPS()
    - void GetOnboardGPSString()
    - void GetGPSTime(char *str, unsigned int size, char *time)
    - void ParseGPSString(unsigned char *str, unsigned int size)
- M02_RadDet.pde: for radiation detection-related functions
    - void SetupRadDet()
    - int GetHit()
- M03_SDmemory.pde: for memory card-related functions
    - void SetupSD()
    - int GetFilename()
    - void WriteEvent()
    - void Reboot()
- M04_Servo.pde: for control of a servo motor
    - void SetupServo()
    - void PointNorth()
    - int ControlServo(float heading)
    - void ServoRotate(Servo *s, float angle)
    - inline float MicrosecondsToAngle(float micro)
    - inline float CheckAngle(float angle)
- M05_eCompass.pde: for electronic compass-related functions
    - void SetupECompass()
    - float GetHeading()
    - void CalibrateCompass()
- M06_HASPSerial.pde: for serial communication-related functions
    - void ReadHASPSerial()
    - void SendHASPSerial()
- M07_TempSensor.pde: for temperature sensor-related functions
    - float GetTemp()

All of these codes were thoroughly tested in the lab and implemented into the microcontroller. During integration, however, it was discovered that the serial port on the Uno32 was using TTL logic levels, whereas the HASP equipment required RS-232 logic levels. In order to enable serial communication, a MAX233 line driver/receiver was additionally installed. After installation, commands could be sent to the payload successfully and science and housekeeping data were received by the HASP instrument, both during integration and flight.

2.5.   Power Module

Most of the onboard modules require a 5Vdc supply to operate, particularly the microprocessor, GPS, SiPM pre-amplifiers, temperature sensor, and rotator. To provide this voltage, a Murata NDY2405C DC-DC converter is used[7]. The e-compass and SD card both required a 3.3V supply, which was provided by the Uno32's built-in, regulated 3.3V supply. The comparator (high gain, large bandwidth OP amp) requires a dual power supply with a maximum differential voltage of 6V. As a result of considering all constraints, a ±2.5V supply was constructed using a second NDY2405C isolated power supply in conjunction with a voltage divider..

Another consideration is the sensitivity of the SiPM gain to the bias voltage. Initially, the HASP 30V power was supplied to the SiPM. However, it was discovered during the HASP instrument integration that the HASP 30 V power supply, which was being used without regulation as the bias voltage for the SiPM units, varied over too wide a range for the SiPM to operate properly. At the upper end of the voltage range (around 32 V), the bias voltage supplied to the SiPM was sufficient to cause continuous triggering on dark noise. This issue was resolved during integration by using an RS-2415DZ regulated DC-DC converter[8], which output a stable ±15Vdc over an 18-36V input range. For the required single power supply, this ±15Vdc dual power supply was wired to produce a 30V single DC output.

3. Experimental Data and Discussions

A photo of the payload in the lab, prior to the final physical integration of all subsystems into a complete payload, is shown in Figure 7. This was the final step of integration testing after rigorous unit testing of all subsystems of the payload was performed. Test equipment included two four-channel oscillopes, two dual-power supplies, two signal generators, and one laptop computer for interface with the microcontroller subsystem.
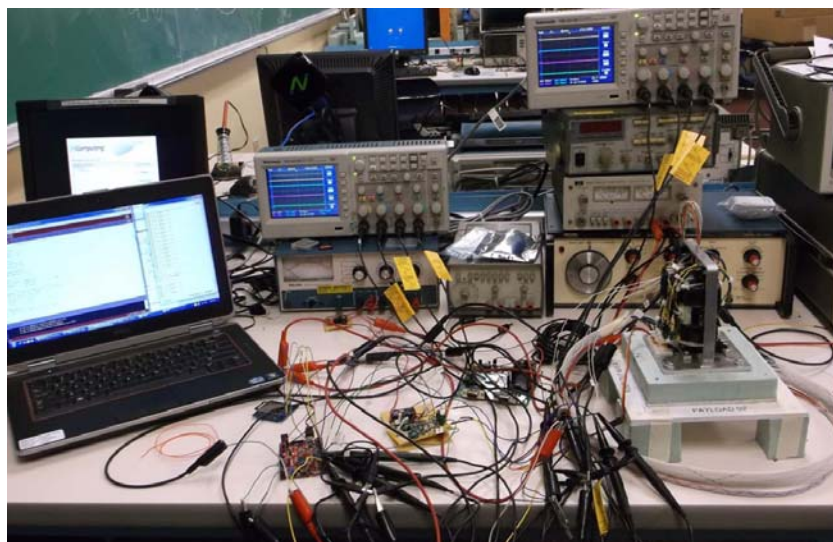
3.1. Lab Testing Data – Detector and Comparator Modules

Figure 7. Setup for lab testing

Selection of properly operating SiPMs was a critical task to ensure operation of the detector module. As such, one of the key test data was the bias voltage of the SiPM, as well as the output signal from the pre-amplifier. In reference to Figure 5, after assembling a green LED, scintillator and pre-amplifier as a detector module, the output voltage of the pre-amplifier was measured. Table 1 shows two test data for 4 detector modules (determined to be properly functioning) among 12 detector modules tested. Test 1 was to determine the maximum possible output from the preamplifier which operates with a 5Vdc power supply. Test 2 was to determine a proper bias voltage for the SiPM on the pre-amplifier board.

Table 1. Testing Data of the Detector Module

Pre-amp board #	Test 1	Test 2
	Preamp Max. Output Voltage [V]	**SiPM Bias Voltage [V]**
	Test condition: Preamplifier input: a 100 kHz pulse signal coupled by C2 = 10 µF; SiPM is not powered (i.e., OFF)	**Test condition**: Preamplifier output: at negative peak voltage < -1V
#4	-2.56	28.2
#5	-2.56	26.2
#8	-2.40	27.6
#10	-2.72	28.0

Figure 8(a) shows an actual pre-amplifier output when all subsystems of the payload were integrated. As shown, the pulse period was about 1.8 µs while its amplitude was 640 mV (not shown). Figure 8(b) shows the comparator output corresponding to the pre-amplifier output. The high gain, high bandwidth OP amp for the comparator was able to successfully process the short negative pulse from the pre-amplifier and produce a positive output of similar duration. The output of ~2.5V (also not shown in the figure) was expected because a ±2.5V dual power supply was used
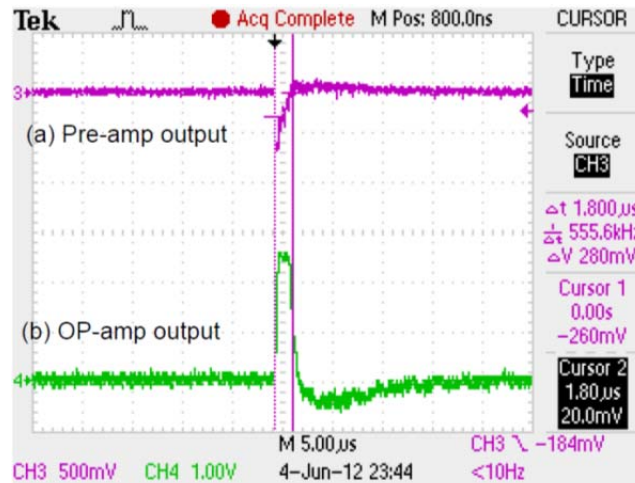

Figure 8. Output signals: (a) pre-amplifier (b) OP amp (comparator)

and the OP amp has an internal configuration of a push-pull class B amplifier. This +2.5 V output exceeded the microcontroller's TTL logic threshold of 2.4 Vdc, and was therefore sufficient to register as a logical "high."

3.2.   In-Flight Experimental Data

Our payload was flight-certified after a 2nd attempt to pass thermal vacuum testing at the CSBF site. The in-flight data shown in Figure 9 ~ Figure 12 was gathered during the HASP 2012 flight through serial communication with the HASP instrument, which was downlinked to a data repository on the ground in real time.

Figure 9 shows the temperature inside the payload. The temperature was monitored to ensure that all subsystems of the payload were operating within an acceptable temperature range, both during thermal vacuum testing and flight. As shown, the temperature was in the range of -20 °C ~ +38 °C except for one data point which shows a temperature of 233 °C (from raw data). Because it would be impossible for the payload to heat and cool so rapidly, it is assumed that the data might have been corrupted during transmission somewhere between the micro-processor serial port and the ground receiver.

Figure 10 shows the payload orientation in reference to the East-West (E-W) plane. The rotator module was used to orient the electronic compass and detector module along the E-W plane. Angular deviations from the reference orientation were measured and corrected when a deviation of more than 10 degrees in either clockwise
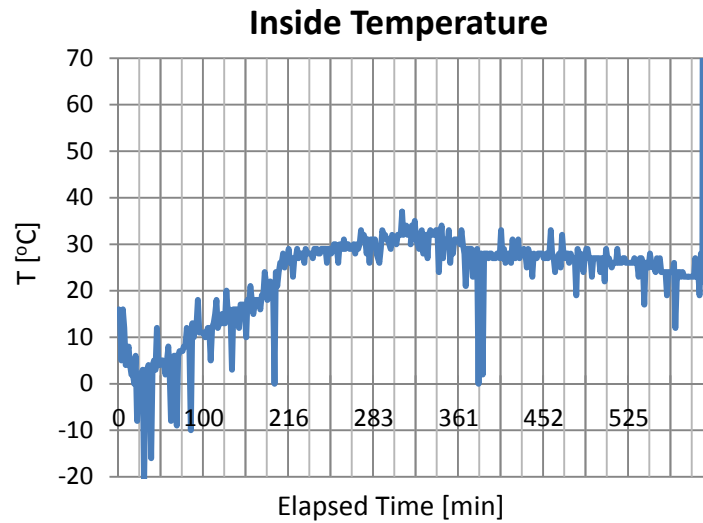

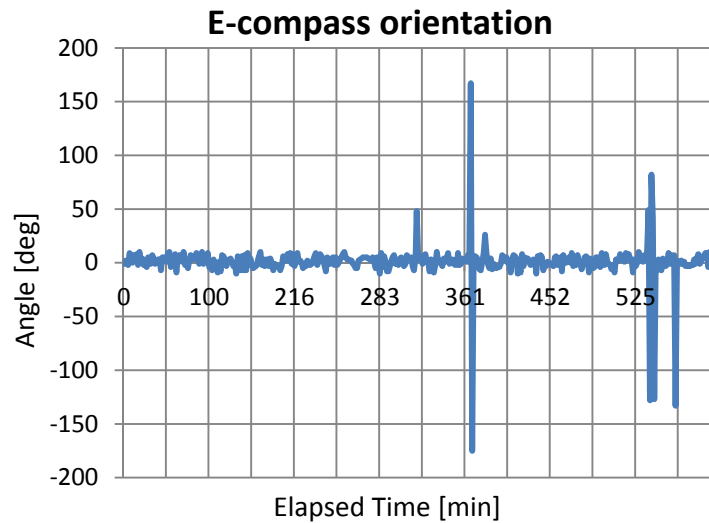**Figure 9. Temperature inside the payload**

Figure 10. Orientation angle [degrees] of the electronic compass referenced to the East-West

(negative) or counter-clockwise (positive) direction occurred. As shown, the payload lost its E-W orientation at some points (e.g., near 361 minutes) but was able to re-align its orientation within the intended orientation error of ±10 degrees. However, sudden changes in angular orientation, e.g., 167 degrees and then 185 degrees (plotted as -175 degrees in the figure) are likely due to the rotator module malfunctioning (e.g. over-correction), as the HASP payload probably did not rotate so quickly.
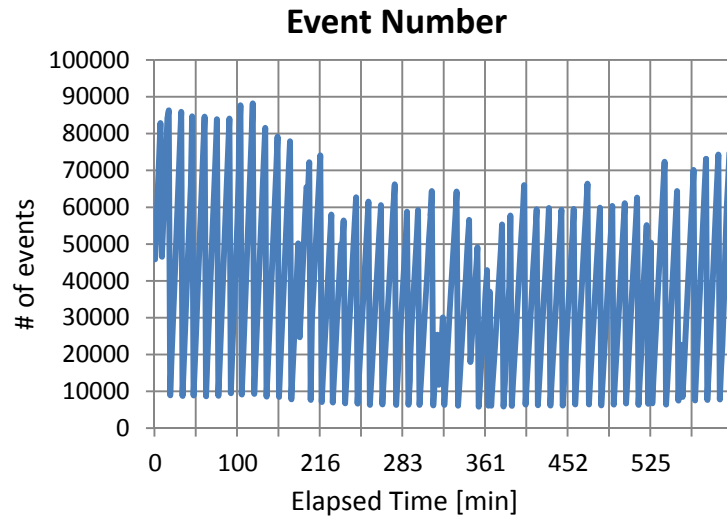
Event Number

Figure 11. Number of coincidence events counted by the Coincidence Module

Figure 11 shows the cumulative event numbers of coincidences. An event is declared when the input voltage to at least two pins of the micro-controller are HIGH, ideally caused by the arrival of a cosmic ray in two separate scintillator modules. The event number should monotonically increase, as the total number of events is accumulating over the flight. This situation can only happen when the micro-controller regularly resets the event number. The most logical explanation is that the microcontroller rebooted itself approximately every 7 minutes, a failure mode not observed in the lab.

Figure 12 shows the event rate, defined as the number of coincidence events per minute, during the flight. The expected event rate was between 10~20 events per minutes. As can be seen, the observed event rate is much higher and is consistent with the instrument triggering constantly.

This failure mode was also observed during the 1st thermal vacuum test. After an apparently unrelated improvement (i.e., addition of an 18~30V-in-30V-out DC-DC converter as discussed above), the event numbers were in the expected range during the 2nd thermal vacuum test, which the payload passed.

4. Failure Mode and Effect Analysis

For potential technical failure modes, some basic concepts of
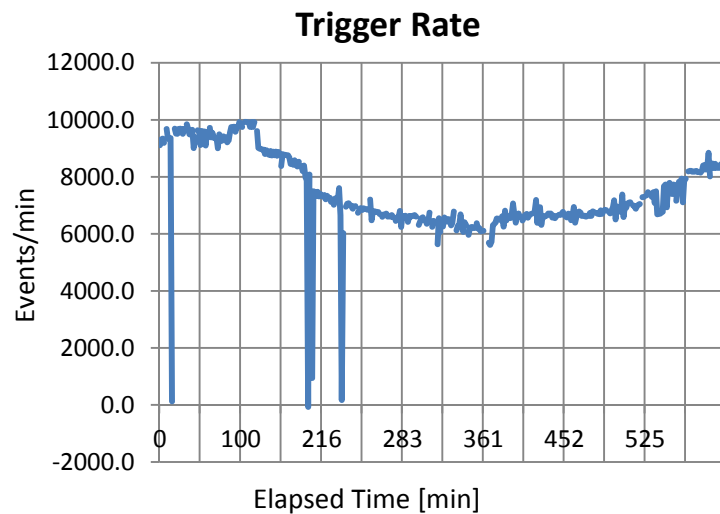
Trigger Rate

Figure 12. Coincidence rate [Events per minute] in all directions

the well-known failure mode and effect analysis (FMEA) can be applied to the payload "system design." As such, rather than tabularizing various factors for the analysis and corrective actions to be taken, as would be done in a formal FMEA, we provide qualitative assessment for further investigation of the possible causes of the subsystem malfunctioning/failure.

Pin-pointing an exact cause is difficult because the failure is not reproducible in the lab. However, based on the observations of experimental data, we assess the potential causes of the problems as follows, and they will be the focus of further improvement of the payload functionality for future flights and in-flight experiments.

SiPM - During the first thermal vacuum test, the detector malfunctioned, essentially triggering continuously. To help resolve this issue, the 18~30V DC-DC converter, described above, was installed and seemed to resolve the problem, as the detector functioned as expected during the second thermal vacuum test and during the pre-flight instrument test. However, for reasons that are still uncertain, the instrument returned to the failure mode observed during the first thermal vacuum test during flight. No usable data was returned from the detector module. It is suggested that the bias threshold shown in Table 1 may need to be set lower as a threshold of ~29V (and slightly adjusted for individual SiPMs by a voltage divider circuit) was used for the detector module in the payload to produce strongest pulses from all SiPMs. A lower bias voltage would produce a weaker pulse that prevents false triggering of the comparator module.

Comparator - The output of the pre-amplifier of the detector module is input to a comparator. Although the original design suggested the comparator voltage be adjustable via an external command, the threshold voltage for the comparator is set to 0 V as it provided adequate results in the lab. Adjusting it to a non-zero threshold had yielded weaker output voltages (less than the desired 2.4 V for TTL logic) from the class B amplifier inside the OP amp for the comparator. As a possible cause of ultimate false event declaration, the application circuit and the circuit board of the comparator would need more attention to remove any design flaws.

Micro-controller - The microprocessor functioned as expected during flight, except that somehow the event numbers were reset regularly. Data were returned to the ground at the expected rate via serial communication, and the temperature and detector orientation remained within expected values most of the time. The GPS timestamp from the onboard GPS was also received, although the GPS timestamp from the HASP instrument was not. However, since the onboard GPS functioned properly, the HASP GPS timestamp was not required. There was a problem with the onboard SD card, however. During shipment, it seems to have jostled out of place, despite being taped into position. Thus, events were not recorded to the SD card during flight. However, the data received via HASP downlink provided redundancy, thus this failure had very little impact on flight success. It is suspected that the overall connections of the subsystems might have caused undesirable triggering or micro-controller rebooting. More attention could possibly be given to the micro-controller code to more aggressively prevent unexpected operation.

Power module – The overall ground level was somewhat unstable, especially when the rotator operated, or a large peak was output from the pre-amplifier (e.g., more than -1.0V). All DC-DC converters would need to be revisited to ensure each of them could cope with an unexpected drawing of a certain level of excessive current from the DC-DC converter.

These qualitative assessments are shared with the student members and efforts are being made for the student team members to refine the payload design for another flight scheduled for Sept 2013 as part of the HASP 2013 campaign.

5. Participants and Assessment of Learning Outcomes

As briefly mentioned earlier, there were six undergraduate students from ECE department. All three seniors (two male and one female student) were involved from the beginning of the project in Fall 2011, and three sophomores (two male and one female student) joined the team during Fall 2011 or in the beginning of Spring 2012. One graduate student was recruited to help the team for a short period of time during the summer 2012.

As the project was carried out as one of the ECE senior design projects, three senior students played a key role in all phases of design activities under close supervision of two faculty advisors of the project. The seniors carried out design activities in and outside of the classroom to fulfill the course requirements and complete assignments for engineering requirements: functional decomposition, project scheduling/milestones and Gantt chart, parts list, and test plan in Fall 2011. The sophomores were brought in to help the seniors in various aspects of the project activities as well as develop interest and familiarity with the project. More serious lab activities actually commenced in Spring 2011 in the second course of the senior design.

For the Spring lab activities, the student team including the sophomores regularly met for about 5 hours of lab work per week, split into two lab sessions, in addition to seniors' own lab activities.

As part of the senior design course, seniors were assessed on some of the key ABET-defined student learning outcomes, such as a) ability to design a system, component, or process to meet desired needs, b) ability to function on multidisciplinary teams, c) understanding of professional and ethical responsibility, d) ability to communicate effectively, and e) recognition of the need for, and an ability to engage in life-long learning. In addition, our ECE department-specific learning outcomes were also assessed, such as i) develop systems containing hardware & software components, and ii) analysis & design of complex electrical & electronic devices. Moreover, some of the liberal arts-related learning objectives set by the University were also assessed, particularly the ability to communicate effectively, both in writing and verbally, and demonstrate successful learning for speech-related objectives including 1) be able to relate the theories and practice of non-verbal communication, 2) recognize and be able to integrate the Aristotelian principles of Ethos, Pathos, and Logos into the performance plan, 3) be able to utilize non-verbal communication strategies (movement, stance, facial expression, and gesture) to enhance the delivered message, and 4) synthesize the use of various vocal techniques to create meaningful messages.

The ABET-defined and ECE department-specific student learning outcomes were assessed based on course-specific deliverables of the senior design course mentioned above, as well as a design specifications document (in the end of the fall semester) and a final project report (in the end of the spring semester). These deliverables are deemed reasonable indicators of effectiveness in student learning. On the liberal arts-related and communication-skill related learning outcomes,

assessments were conducted based on student team's participation in various formal oral presentations and written reports. Oral presentations were offered at least twice a semester within the department, including final oral presentations in fall and spring semesters. An IEEE student paper competition was conducted in the spring with external judges as part of the preparation for IEEE Region 2's Student Activities Conference.

The students' performance was more than average when all projects in their class were considered, and the team won the first place in an internal project competition and went on with a student paper to represent the IEEE branch at the University in a regional IEEE student conference. For the sophomores, no formal assessment was conducted as their involvement was primarily for developing interests in undergraduate research and to prepare them for leadership roles in future endeavors.

6. Lessons Learned

This project provided a great framework for undergraduate students in research and enhancing their learning experience. One of the challenges in carrying out the overall project activities was time management amid student's busy schedule, as undergraduate students normally carry 15~18 credit hours of coursework as well as their extracurricular activities. At times, students lost motivation to complete project activities, especially when obstacles arose and progress in their responsible subsystems was slower than they expected. Keeping them motivated through encouragement and weekly meetings was crucial for successful completion of the project by a set-deadline.

Students are learners, as opposed to being experts, and often were not dedicated to the concept of "deliver" that is one of the essential skills of the real-world work place. As such, faculty advisors' technical guidance and hands-on work with students in the lab was frequently required.

Students' travel to an off-campus site for intercollegiate collaboration, i.e., integration of the payload into the HASP at the CSBF site, was a great way to enhance their overall learning experience and enthusiasm for this project.

7. Concluding Remarks

We have presented design details of a student design project, key experimental data, and lessons learned from and during the course of the project. Although the payload failed to collect the desired cosmic-ray data, all other parts of the design, including serial communications, payload orientation, and temperature monitoring, functioned as expected. Additionally, this project provided student team members with an engineering opportunity that requires technical and also non-technical skills to solve real-world problems. This project was adopted as a senior design project for the 2011-2012 academic year with three of the design team members participating as seniors in the ECE department. As such, this project was a considerable success from a student education standpoint. The payload can serve as a framework for student design projects in an on-going basis. With refinements and modifications of the payload design and functionality, a standalone small-scale balloon system could be launched to carry the payload to near space, supported by a track-and-recover system available in the ECE department.

References

[1] High Altitude Student Platform: Call for Payloads 2012, issued by Dept. of Physics at Louisiana State University, Baton Rouge, LA, and Balloon Program Office at NASA Wallops Flight Facility, Wallops Island, VA, October 2011.

[2] Photoniques SA, 1.3mm2 active area, low noise solid state photomultiplier for visible and near-IR light applications, Data sheet, Doc. No.: SSPM_0905V13MM, September 2009.

[3] Application circuit diagram for AMP-0604 and AMP-0611, Photoniques SA, available on line at http://www.photonique.ch/Prod_AMP_0600.html.

[4] Honeywell, Digital Compass Solution HMC6352, data sheet, available on line at https://www.sparkfun.com/products/7915.

[5] Analog Devices, AD8615/AD8616/AD8618: Precision, 20 MHz, CMOS, Rail-to-Rail Input/Output Operational Amplifiers, data sheet, 2008.

[6] Digilent, chipKIT™ Uno32™ Board Reference Manual, Doc: 502-209, October 25, 2011.

[7] Murata NDY2405C, NDY Series: Isolated 3W Wide Input DC/DC Converters, data sheet, Doc. No.: KDC_NDY.F02, 2012.

[8] Recom Power, RS-2415DZ, ECONOLINE DC/DC-Converter, REV: 0/2012.